LA-UR-97-2276

CONF-970745--1

Los Alamos National Laboratory is operated by the University of California for the United States Department of Energy under contract W-7405-ENG-36

TITLE: **ON THE MODELING OF THE TAYLOR CYLINDER IMPACT TEST FOR ORTHOTROPIC TEXTURED MATERIALS: CALCULATIONS AND EXPERIMENTS**

AUTHOR(S): Paul J. Maudlin, Theoretical Division, T-3
John F. Bingert, MST-6
Joel W. House, Eglin AFB

SUBMITTED TO: *International Symposium on Plasticity, Juneau, Alaska, July 14–17, 1997*

Los Alamos National Laboratory
Los Alamos, New Mexico 87545

DISCLAIMER

On the Modeling of the Taylor Cylinder Impact Test for Orthotropic Textured Materials: Calculations and Experiments

Paul J. Maudlin*, John F. Bingert, and Joel W. House

*Mail Stop B216
Los Alamos National Laboratory
P. O. Box 1663
Los Alamos, NM 87545

Taylor impact tests using specimens cut from a rolled plate of Ta were conducted. The Ta was well-characterized in terms of flow stress and crystallographic texture. A piece-wise yield surface was interrogated from this orthotropic texture, and used in EPIC-95 3D simulations of the Taylor test. Good agreement was realized between the calculations and the post-test geometries in terms of major and minor side profiles and impact-interface footprints.

INTRODUCTION

Impact calculations involving metals are usually performed using strength constitutive models that assume isotropy. This assumption usually takes the form of an isotropic elastic stiffness tensor, a realistic flow stress model and a von Mises yield function. Real materials deviate from isotropy both in elasticity and plasticity. The calculations described here relax these assumptions by utilizing an anisotropic elastic stiffness tensor and an anisotropic representation of the yield surface, in particular a piece-wise surface tessellated from direct measurements of the crystallographic texture. This effort validates the use of such constitutive modeling by comparing calculations to measured geometric shapes of post-impact Taylor [1948] cylinder specimens for a Ta material.

TAYLOR CYLINDER TESTS

Consider a plate (Fig. 1a) of Ta (Cabot material, referred to here as DoD Ta) received from NSWC, White Oak Detachment, for which mechanical characteriztion was performed in terms of flow stress behavior by Chen [1996] and crystallographic texture. The manufacturing process for this plate produced the near-orthotropic rolling texture shown in Fig. 1b. These equal-area pole figures are recalculated from an orientation distribution (OD). The OD was derived from the {100}, {200}, and {211} x-ray experimental pole figures, interrogating the 2'-3' plane.

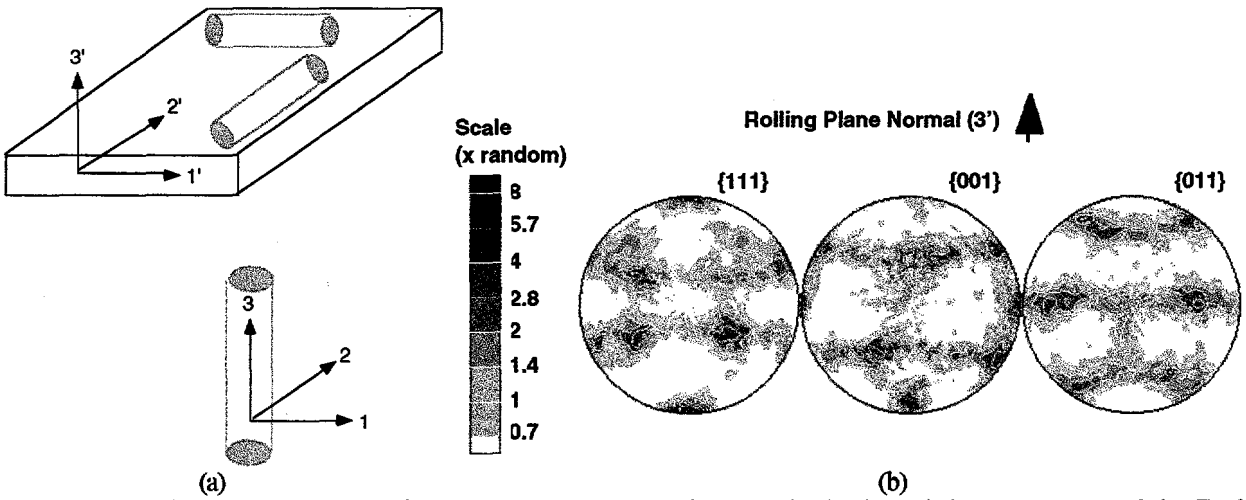

Figure 1: (a) Schematic of a Ta plate showing the material axes (1', 2', 3') and the orientation of the Taylor cylinder test specimens relative to the plate. (b) Recalculated x-ray equal-area pole figures for the DoD Ta plate measured over an areal patch on the 2'-3' plane indicated in Fig. 1a.

Taylor [1948] cylinder impact specimens were cut from the Ta plate in the 1' and 2' orientations as shown in Fig. 1a, i.e., the cylinder centerlines are coincident with either the material 1'-axis, or the 2'-axis. The specimens were caliber 30 (7.62 mm diameter) cylinders with a length of 1.5 inch (38.1 mm) giving a L/D = 5. The laboratory test frame (axes 1, 2, 3) attached to the Taylor specimens as shown in Fig. 1a, represents the principal axes of the impact test such that the compression loading is always applied along the 3-axis (i.e., the specimen centerline).

The Taylor specimens were tested at Eglin Air Force Base producing three good post-test geometries (designated SC-11, SC-12 and SC-21). The cylinders were launched using a caliber 30 Mann powder gun. The velocity of the projectiles was measured by both pressure transducers and parallel laser beams crossing the flight path. Velocities determined from the two systems were about 175 m/s, agreeing to within ± 3.0 m/s. The anvil target was 4340 steel heat treated to a surface hardness of Rc 58. After testing, profile geometric data for the deformed specimens was generated using an optical comparitor. The data consist of three digitized side profiles for the minor dimension (see Fig. 2a), same for the major dimension (see Fig. 2a), and three digitized footprints that give the 1-2 cross-sectional area at the impact interface (see Fig. 2b).

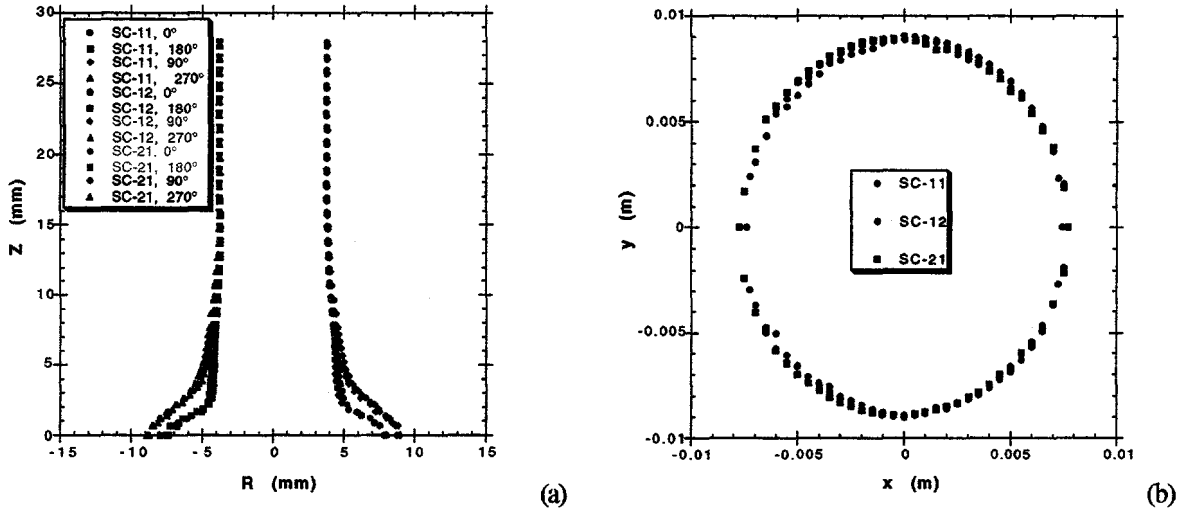

Figure 2: (a) Digitized minor (0° and 180°) and major (90° and 270°) side profiles and (b) footprints of three post-test geometries for Ta Taylor specimens SC-11, SC-12 and SC-21.

CONSTITUTIVE MODELING

For the mechanical response, the MTS flow stress model as described and characterized for the DoD Ta by Chen [1996] in conjunction with the multisurface plasticity algorithm described by Maudlin [1996] using the piece-wise yield surface given by Fig. 3 was used. A Ta orthotropic elastic stiffness tensor also given by Maudlin [1996] and a Mie-Gruniesen equation-of-state were also used as part of the constitutive modeling. Note that the MTS flow stress model is an internal state variable model, nominally a function of strain, strain-rate and temperature, and has been previously implemented in the baseline version of EPIC-95.

Applying the ODF probing procedure described by Maudlin [1996] to the rolling texture shown in Fig. 1b, the 5D piece-wise yield surface shown in Fig. 3 was produced, cast in the material frame coordinates shown in Fig. 1a (axes 1', 2', 3'). Orthotropic symmetry and sign-independence were assumed in the supporting LApp (Los Alamos polycrystal plasticity) strain-probe calculations; thus only half of the π-plane and one octant of the shear subspace were probed.

The 2D π-plane subspace (left side of Fig. 3) is a yield surface section where the shear stresses are all zero. The round symbols in this figure are the LApp-probed yield stresses, tessellated together with 2D linear functions. The largest average Taylor factor $\overline{M}$ for this Ta piece-wise curve is 2.898. A von Mises yield function plotted in the Fig. 3 π-plane would be a circle of radius $\overline{M} = 2.898$ if the flow stress σ had been characterized in the 3' direction.

The 3D shear subspace (right side of Fig. 3) is another yield surface section where the normal stress components are zero. The triangular vertices on this surface are LApp-probed yield stresses that are tessellated together with 3D linear functions. A von Mises yield function plotted in the Fig. 3 shear subspace would be a sphere of radius $\overline{M}$ = 2.898 if again σ had been characterized in the 3' direction.

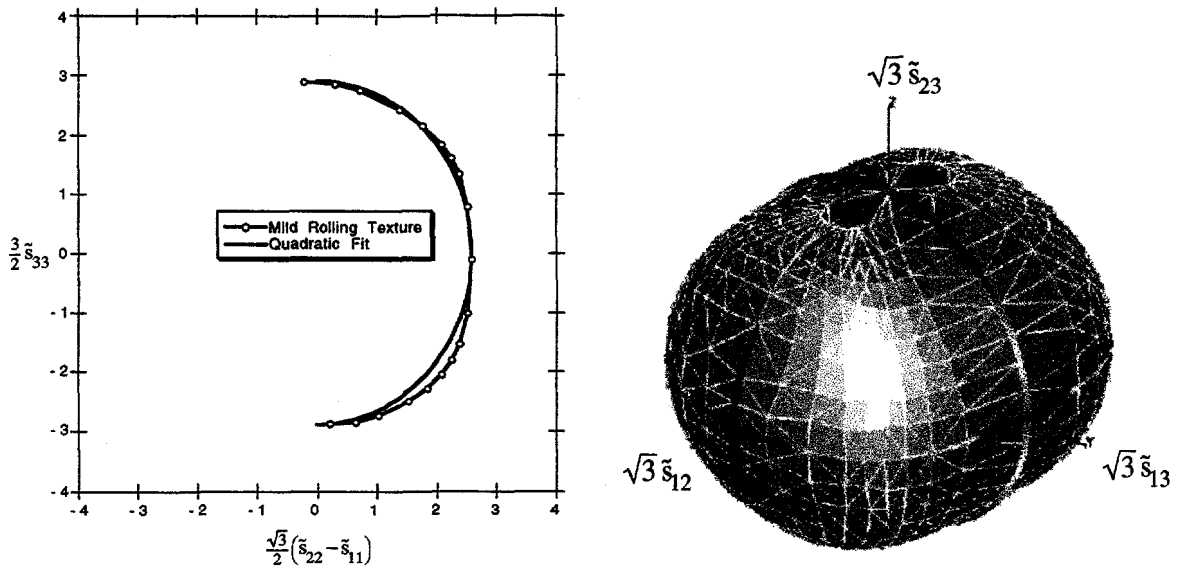

Figure 3: A two-dimensional p-plane subspace (left) showing a piece-wise (DoD Ta plate) yield surface (line segments and points) being compared with a quadratic fit (solid curve) interpolating the piece-wise function at the horizontal and vertical axis intercepts. Also shown is the associated three-dimensional shear subspace perspective (right) of the piece-wise yield surface (3D triangular facets) being compared with a quadratic fit (solid curves in each plane) interpolating the piece-wise function at the x, y, z axis intercepts.

The curves appearing in the π-plane and the x-y, x-z, and y-z planes of the shear subspace illustrate the goodness of a Hill [1950] quadratic fit, i.e., in deviatoric stress s_{ij} cast in the material frame:

$$f \equiv \frac{1}{2}\left[(G+H)\tilde{s}_{11}^2+(F+H)\tilde{s}_{22}^2+(F+G)\tilde{s}_{33}^2-2H\tilde{s}_{11}\tilde{s}_{22}-2G\tilde{s}_{11}\tilde{s}_{33}-2F\tilde{s}_{22}\tilde{s}_{33}\right] + N\tilde{s}_{12}^2+M\tilde{s}_{13}^2+L\tilde{s}_{23}^2-\frac{1}{3}\overline{M}^2=0 \quad (1)$$

to the piece-wise yield function for this Ta material. Observe from Figs. 3 that the analytical fit captures the basic shape of this yield surface but misses some topographic features (stress corners and flat spots). Coefficients for this Ta quadratic fit in Hill [1950] form are:

$$(F,\ G,\ H,\ L,\ M,\ N)=(1.000,\ 1.000,\ 1.375,\ 5.164,\ 4,573,\ 3.581) \quad (2)$$

The π-plane of Fig. 3 and the coefficients of Eqn. (2) indicate that the 3' through-thickness direction is the so-called "strong" direction for the Ta plate (maximum distance between the stress origin and the yield curve), and the "weaker" 1' and 2' directions are both comparable in terms of strength as indicated by the coefficients F and G in Eqn. (2). This is also evident in the texture data of Fig. 1b which reveals a concentration of the strong <111> crystallographic direction aligned parallel to the 3' direction.

TAYLOR IMPACT SIMULATIONS AND COMPARISONS

Assuming isotropic strength (or anisotropic strength with transverse isotropy), a Taylor cylinder impact event is an axisymmetric problem that can be simulated with a 2D continuum code. However, with the introduction of a

directionally dependent constitutive description, e.g., including an orthotropic yield surface such as Fig. 3, the Taylor problem will exhibit three-dimensional deformation requiring a 3D code for simulation. Hence the specific Taylor cylinder tests described above were simulated with the explicit Lagrangian continuum mechanics code EPIC in a 3D mode under the assumptions of negligible impact-interface friction and anvil compliance. The cylinder was spatially modeled using 4185 nodes and 17,280 single-integration-point tetrahedral elements (in symmetrical arrangement). The impact event was simulated for 80 μs of problem time after which plastic deformation is insignificant.

Calculated meshes in Fig. 4 show late-time cylindrical major and minor side profiles and an impact-interface footprint that are all compared with the experimental shapes (as circular points) from Figs. 2. The calculated elliptical footprint shown in Fig. 4 has an eccentricity (E = ratio of major to minor diameters) that compares well to the experimental footprints from Fig. 2b; a von Mises function would produce a round footprint (E = 1).

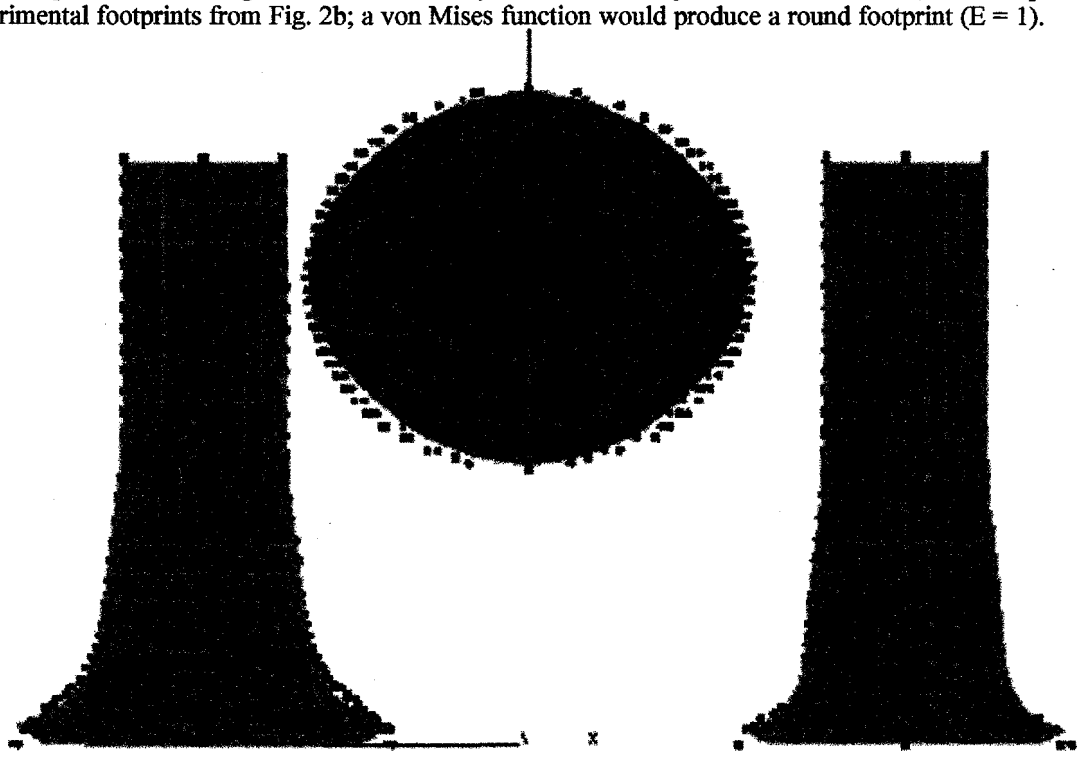

Figure 4: Comparison of Taylor cylinder impact simulation results showing major and minor side profiles and the impact-interface footprint at late-times with digitized experimental post-test shapes from three shots. The saturation threshold stress in the MTS model was reduced by 10% to decrease the effect of work hardening to achieve these results.

The axial distribution of plastic strain in a Taylor test is essentially determined by the flow stress model. The good comparison in side profiles shown in Fig. 4 was achieved after reducing the saturation flow stress at zero degrees K $\hat{\sigma}_{so}$ from its value given by Chen [1996] of 645 MPa to 580 MPa. This has the effect of reducing the magnitude of the threshold stress $\hat{\sigma}$ evolved at large strains and decreases the work hardening in the "foot" region of the cylinder at the anvil face. Prior to reducing $\hat{\sigma}_{so}$ the computed post-geometry length agreed well with the experimental shape, but the axial distribution of plastic strain was overly concentrated in the "bulge" volume above the foot. All other MTS parameters from Chen [1996] for this DoD Ta and the piece-wise yield surface given by Fig. 3 were used unaltered for the Fig. 4 simulation.

REFERENCES

[1948] G. I. Taylor, *Proc. Roy. Soc. London,* **A-194,** 289.
[1950] R. Hill, The Mathematical Theory of Plasticity, Oxford University Press, London.
[1996] S. R. Chen and G. T. Gray III, *Met. Trans.* **27A,** 2994-3006.
[1996] P. J. Maudlin, S. I. Wright, U. F. Kocks and M. S. Sahota, *Acta mater*, **44,** Number 10, 4027-4032.